Geophysical Research Letters

Supporting Information for

Modelling the impacts of future enhanced winter warming events on subarctic ecosystem using LPJ-GUESS

D. Pascual[1*], M. Johansson[1], A. Pongracz[1], & J. Tang[1,2]

[1]Department of Physical Geography and Ecosystem Science, Lund University, Lund Sweden

[2]Section of Terrestrial Ecology, Department of Biology, University of Copenhagen. Copenhagen, Denmark

[*]Corresponding author. E-mail: Didac.pascual@nateko.lu.se - Affiliation address: Sölvegatan 12, 223 62 Lund, Sweden - Telephone dir 0046 720324595

Contents of this file

Introduction

The Supporting information for this article contains the following information:

- A: a detailed description of the plant functional types and their parameterization.
- B: additional descriptions of the input data.
- C: detailed descriptions of the global climate model data used for the creation of the winter warming event scenarios, further details of the methods employed to create such scenarios, and an overview of the anomalies applied to create such scenarios.
- D: further details regarding the methods and the results of the Sensitivity Analysis.
- E: a list of the model evaluation data, and figures supporting the descriptions provided in the manuscript regarding the results of the model evaluation.
- F: additional figures to visualize the results of the study described in the main manuscript.

A. Plant functional types (PFT's) simulated for the four ecosystem types investigated

Table A1. Full details of the Plant Functional Types (PFTs) and typical species simulated in the different ecosystem types. Superscripts 1, 2, 3, and 4, denote each PFT belonging to the birch forest, tundra, peat plateau, and fen sites, respectively.

PFT name	Typical species
IBS [1] (Shade-intolerant broadleaved summergreen tree)	Betula pubescens
LSE [1,2] (Low evergreen shrub)	Empetrum hermaphroditum Juniperus communis, Vaccinium vitis-idaea; Andromeda polifolia
LSS [2] (Low summergreen shrub)	Vaccinium myrtillus, V. uliginosum, Salix hastata, S. glauca etc.
EPDS [2] (Prostrate evergeeen dwarf shrubs)	Vaccinium oxycoccus, Cassiope tetragona, Dryas octopetala, Saxifraga oppositifolia
SPDS [2] (Prostrate summergreen dwarf shrub)	Salix arctica, Arctostaphylos alpinus, Salix reticulata
pLSE [3] (peatland low evergreen shrub)	Vaccinium vitis-idaea, Cassiope tet.,
pLSS [3] (peatland low summergreen shrub)	Vaccinium myrtillus, V. uliginosum, Salix hastata, S. glauca
GRT [2] (Graminoid and forb tundra)	Artemisia, Kobresia, Brassicaceae
CLM [1,2] (cushion forb, lichen and moss tundra)	Saxifragacea, Caryophyllaceae, Papaver, Draba, lichens, mosses
pCLM [3] (peatland cushion forb, lichen and moss tundra)	Saxifragacea, Caryophyllaceae, Papaver, Draba, lichens, mosses
WetGRS [3] (cool, flood-tolerant grass)	Carex spp., Eriophorum spp., Juncus spp., Typha spp.
pmoss [3,4] (peatland moss)	Sphagnum spp.

Table A2. Full descriptions of the PFT parameters for the four ecosystem types investigated (birch forest, tundra, peat plateau, and fen). IBS: shade-intolerant broadleaved summergreen tree; LSE: low shrubs evergreen; LSS: low shrubs summergreen; EPDS: evergreen prostrate dwarf shrubs; SPDS: summergreen prostrate dwarf shrubs; pLSE: peatland low shrubs evergreen; pLSS: peatland low shrubs summergreen; GRT: graminoid tundra; CLM: cushion forbs, lichens and mosses tundra; pCLM: peatland cushion forbs, lichens and mosses tundra; WetGRS; cool, flood-tolerant grass; pmoss: peatland moss; NL: needleleaf; BL: broadleaf; Max.: maximum; Min.: minimum; EG: evergreen; SG: summergreen; GDD5: growing degree days above 5 °C; GDD0: growing degree days above 0 °C.

Parameters	**Abbreviation in LPJ-GUESS**	**IBS** [1]	**LSE** [1,2]	**LSS** [2]	**EPDS** [2]	**SPDS** [2]	**pLSE** [3]	**pLSS** [3]	**GRT** [2]	**CLM** [1,2]	**pCLM** [3]	**WetGRS** [3,4]	**pmoss** [3,4]
Growth form		Tree	Shrub	Shrub	Shrub	Shrub	Shrub	Shrub	Grass	Grass	Grass	Grass	moss
Leaf physiognomy		BL	NL	BL	NL	BL	NL	BL	BL	BL	BL	BL	BL
Fraction of roots in the upper/lower soil layer	**rootdist**	0.6/0.4	0.8/0.2	0.8/0.2	0.8/0.2	0.8/0.2	0.8/0.2	0.8/0.2	0.9/0.1	0.9/0.1	0.9/0.1	0.9/0.1	1
Max. Leaf:root C mass ratio	**ltor_max**	1	1	1	0.5	0.5	1	1	0.2	0.2	0.4	0.2	0.1
Min. Canopy conductance (mm/s)	**gmin**	0.5	0.3	0.5	0.5	0.5	0.3	0.5	0.5	0.5	0.5	0.5	0.1
Phenology types	**phenology**	SG	EG	SG	EG	SG	EG	SG	any	any	any	any	any
Longevity of leaves(years)	**leaflong**	0.3	3	0.5	3	0.5	3	0.5	0.5	0.5	0.5	0.5	1
Leaf turnover rate ($year^{-1}$)	**turnover_leaf**	1	0.33	0.7	0.5	1	0.33	0.7	1	1	0.6	1	1
Root turnover rate ($year^{-1}$)	**turnover_root**	0.7	0.7	0.7	0.7	0.7	0.7	0.7	0.5	**0.7**	0.5	0.5	0.5
Sapwood turnover rate ($year^{-1}$)	**turnover_sap**	0.1	0.01	0.01	0.01	0.01	0.01	0.01	-	-	-	-	-
Fire resistance(0-1)	**fireresist**	0.1	0.12	0.12	0.12	0.12	0.12	0.12	0.5	0.5	0.5	0.5	0.5
Min. Forest floor PAR establishment ($J/m^2/day$)	**parff_min**	3500000	1000000	1000000	1250000	1250000	1000000	1000000	1250000	1250000	1250000	1250000	1000000
Interception coefficient	**intc**	0.02	0.06	0.02	0.04	0.02	0.06	0.02	0.01	0.01	0.01	0.01	0.01
Parameter for relationship between crown area and stem diameter	**k_allom1**	250	10	10	10	10	10	10	-	-	-	-	-
Allometry parameter related to vegetation height and stem diameter	**k_allom2**	60	4	4	1	1	4	4	-	-	-	-	-
Allometry parameter related to vegetation height and stem diameter	**k_allom3**	0.67	0.67	0.67	0.67	0.67	0.67	0.67	-	-	-	-	-
Constant in crown area and stem diameter relationship	**k_rp**	1.6	1.6	1.6	1.6	1.6	1.6	1.6	-	-	-	-	-
Maximum tree crown area (m2)	**crownarea_max**	50	1	1	1	1	1	1	-	-	-	-	-
Tree leaf to sapwood area ratio	**k_latosa**	6000	125	125	100	100	125	125	-	-	-	-	-

Sapwood and heartwood density (kgC/m3)	**wooddens**	200	250	250	200	200	250	250	-	-	-	-	-
Growth efficiency threshold (kgC/m2leaf/yr)	**greff_min**	0.04	0.012	0.012	0.01	0.01	0.012	0.012	-	-	-	-	-
Max. Establishment rate (samplings/m2/yr)	**est_max**	0.2	0.75	0.8	0.8	0.8	0.35	0.8	-	-	-	-	-
Recruitment shape parameter	**alphar**	10	10	10	10	10	10	10	-	-	-	-	-
Mean non_stress longevity	**longevity**	300	25	25	30	30	25	25	-	-	-	-	-
GDD5 ramp for phenology	**phengdd5ramp**	190	0	50	0	50	0	50	50	1	1	100	75
Photosynthesis min temperature (ºC)	**pstemp_min**	-4	-4	-4	-4	-4	-4	-4	-4	-4	-4	-5	-4
Approximate lower range of temperature optimum for photosynthesis	**pstemp_low**	10	10	10	10	10	10	10	10	10	10	5	10
Aproximate upper range of temperature optimum for photosynthesis	**pstemp_high**	25	25	25	20	20	25	25	25	25	25	30	30
Photosynthesis max temperature (ºC)	**pstemp_max**	38	38	38	38	38	38	38	38	38	38	45	38
Min. Temperature of coldest month for survival	**tcmin_surv**	-30	-32.5	-40	-1000	-1000	-32.5	-40	-1000	-1000	-1000	-1000	-1000
Min. Temperature of coldest month for establishment	**tcmin_est**	-30	-32.5	-40	-1000	-1000	-32.5	-40	-1000	-1000	5	-1000	-1000
Max. Temperature of coldest month for establishment	**tcmax_est**	3	1000	1000	1000	1000	1000	1000	1000	1000	1000	1000	15.5
Min. Temperature of warmest month for establishment	**twmin_est**	-1000	-1000	-1000	-1000	-1000	-1000	-1000	-1000	-1000	-1000	-1000	-1000
Min. GDD5 for establishment	**gdd5min_est**	350	100	100	0	0	75	100	100	0	0	0	0
Min. GDD0 for reproduction	**zero_min**	500	300	300	150	150	300	300	500	50	50	150	0
Max. GDD0 for reproduction	**zero_max**	-	-	-	1500	350	-	-	1000	150	150	150	5000
Min. Snow cover (mm)	**min_snow**	-	-	-	20	20	-	-	-	50	50	-	-
Maintenance respiration coefficient	**respcoeff**	1	1	1	1	1	1	1	1	1	1	1	2
Min. fraction of available soil water in upper soil layer in the growing season	**drought_tolerance**	0.46	0.1	0.1	0.01	0.01	0.1	0.1	0.01	0.01	0.01	0.01	1
Maximum water table position for establishment (mm)	**wtp_max**	-301	-301	-301	-301	-301	-250	-250			-200	100	0
Max. inundation duration (days) before GPP is reduced to 0	**inund_duration**	-	-	-	-	-	5	5	-	-	31	31	15
Max. evapotranspiration rate	**emax**	5	5	5	5	5	5	5	5	5	5	5	1
Litter moisture flammability threshold (fraction of AWC)	**litterme**	0.3	0.3	0.3	0.3	0.3	0.3	0.3	0.2		0.2	0.2	0.2

Sapwood C:N mass ratio	**cton_sap**	330	330	330	300	300	330	330	-	-	-	-	-
Fine root C:N mass ratio	**cton_root**	29	29	29	29	29	29	29	29	29	29	29	50
Maximum nitrogen uptake per fine root [kgN kgC-1 day-1]	**nuptoroot**	0.003	0.0028	0.0028	0.00551	0.00551	0.0028	0.0028	0.00551	0.00551	0.00551	0.00551	0.00551
Half-saturation concentration for N_uptake [kgN L-1]	**km_volume**	1.5E-06	1.5E-06	1.5E-06	1.5E-06	1.5E-06	1.5E-06	1.5E-06	1.9E-06	1.9E-06	1.9E-06	1.9E-06	1.9E-06
Fraction of sapwood or root (for herbaceous PFTs) for N longterm storage	**fnstorage**	0.15	0.3	0.3	0.3	0.3	0.3	0.3	0.3	0.3	0.3	0.3	0.3
Isoprene emission capacity (ug C g-1 h-1)	**eps_iso (I_{S30}/I_{S20})***	45	1.737	6.85	1.4	14.003	1.737	2	9.818	1.198	1.29	1.198	1.2
Isoprene emissions show a seasonality (1) or not(0)	**seas_iso**	1	0	1	0	1	0	1	1	0	0	0	0
Monoterpene emission capacity (ug C g-1 h-1)	**eps_mon (M_{S30}/M_{S20})***	0.52/0.08	0.088	0.748	1.301	0.425	0.088	0.748	0	0	0	0	0
Fraction of monoterpene production that goes into storage pool	**storfrac_mon**	0.4	0.5	0.5	0.5	0.5	0.5	0.5	0.5	0	0	0	0
Aerodynamic conductance (m s-1)	**ga**	0.04	0.04	0.04	0.03	0.03	0.04	0.04	0.03	0.03	0.03	0.03	0.03

1 Denotes PFT's belonging to the birch forest site. 2 Denotes PFT's belonging to the tundra site. 3 Denotes PFT's belonging to the peat plateau site. 4 Denotes PFT's belonging to the fen site.

B. Extended description of the input data

Four gaps in daily radiation data from ANS (1 January–30 June 1984, 9–16 June 2016, 13–15 February 2007, 23 July–17 August 2011) were filled with the Princeton reanalysis dataset (Sheffield et al., 2006) for the grid cell nearest Abisko. Given their vicinity and similar elevation (altitudinal range <100 m), the birch forest, peat plateau, and tundra sites were run with climate data from the ANS data set (1913-2018; ANS 2020), whereas the fen site used data from Katterjokk Station (1973-2018; SMHI) and bias-corrected daily data (1913-1972) from the ANS.

C. Full details of the WWE manipulation experiments

We selected six CMIP6 climate scenarios from two general circulation models (GCMs) with different climate sensitivities, i.e., CanESM5 and GFDL-ESM4, and three shared socioeconomic pathways representing three levels of varying greenhouse gas projections, i.e., SSP119, SSP270, and SSP585. The SSPs are narratives describing how global society, demographics, and economics could change over this century, and whether and how different radiative forcing levels (Representative Concentration Pathways, or RCPs) can be reached under these narratives (Riahi et al., 2017). The resulting scenario names are a combination of the SSP narratives and the RCP radiative forcings, and include a broad range of scenarios in which mitigation and adaptation challenges vary from low to very high (SSP119: SSP1 and SSP585: SSP5, with the radiative forcing reaching 1.9 and 8.5 W m^{-2} respectively at the end of this century).

For each scenario (n=6), daily meteorological data (1950-2100) for the gridcell near the Torneträsk area was extracted, and then bias-corrected at daily scale against the observed meteorological data using the period 1985-2014, based on the method described in Hawkins et al., (2013). Since GCMs tend to overestimate the number of low-magnitude rain events as compared to observations (Gutowski et al., 2003), precipitation events below a certain threshold (1.5 mm and 1 mm for the ANS and Katterjokk Station data, respectively) were removed in the GCM's output before bias-correction to realistically match the observed wet-day frequency at each site.

Table C1. The four WWE indices used to create the WWE manipulation experiments S1, S2, and S3. The indices were computed using mean daily air temperature (T) and daily precipitation sum (P). Adapted from Vikhamar-Schuler et al. (2016).

Index Number	Name	Description
1	Frequency of melt days	T > 0°C
2	Intensity of melt days	$\sum_{days=1}^{n} (T > 0°C)$
3	Frequency of ROS	T > 0°C, and P > 1 mm
4	Intensity of ROS	$\sum_{days=1}^{n} (T > 0°C, \; and \; P > 1 \; mm)$

Table C2. Full details of the monthly anomalies in each of the four WWE indices and each of the six CMIP6 scenarios from the Abisko Station and Katterjokk Station datasets, calculated for November to March based on the periods of 2071-2100 and 1985-2014.

		WWE anomalies for the Abisko dataset					WWE anomalies for the Katterjokk dataset				
WWE index	**CMIP6 scenario**	**January**	**February**	**March**	**November**	**December**	**January**	**February**	**March**	**November**	**December**
Index 1. Melt days	CanESM5 SSP119	2	2	1	8	5	2	2	0	8	4
	CanESM5 SSP270	6	3	7	15	13	6	2	4	14	12
	CanESM5 SSP585	11	8	12	20	20	11	7	9	21	19
	GFDL-ESM4 SSP119	1	0	0	2	0	1	0	-1	1	0
	GFDL-ESM4 SSP270	2	1	1	4	2	2	1	1	4	2
	GFDL-ESM4 SSP585	6	2	4	11	5	6	2	4	10	5
Index 2. Positive degree days (°C)	CanESM5 SSP119	1.9	2.6	1.3	32.7	12.2	1.7	2.0	0.7	26.7	9.5
	CanESM5 SSP270	11.3	3.3	9.4	57.0	34.0	10.7	2.5	4.8	45.5	26.7
	CanESM5 SSP585	25.2	12.1	24.7	119.3	80.2	24.0	9.6	15.2	103.2	68.9
	GFDL-ESM4 SSP119	0.7	0.6	-1.3	4.2	-0.4	0.7	0.5	-0.8	3.2	-0.6
	GFDL-ESM4 SSP270	2.6	1.0	2.1	15.6	3.9	2.4	0.8	1.3	12.5	2.7
	GFDL-ESM4 SSP585	12.5	3.1	9.8	40.3	10.6	11.9	2.4	6.3	32.0	7.8
Index 3. Melt and precipitation days	CanESM5 SSP119	1	1	0	3	2	1	1	0	5	3
	CanESM5 SSP270	3	1	3	5	5	4	1	2	8	6
	CanESM5 SSP585	5	3	4	7	7	7	4	5	11	10
	GFDL-ESM4 SSP119	1	0	-1	1	0	1	0	-1	1	1
	GFDL-ESM4 SSP270	1	1	0	2	1	1	1	0	3	2
	GFDL-ESM4 SSP585	4	1	2	5	3	5	1	3	7	3
Index 4. Cumulative rain during Index 3 (mm)	CanESM5 SSP119	2.9	3.4	0.9	10.1	2.6	8.8	9.7	1.3	36.8	10.3
	CanESM5 SSP270	8.2	3.1	6.5	12.8	11.8	24.8	8.1	15.1	47.1	37.0
	CanESM5 SSP585	12.8	9.8	10.2	19.7	22.1	40.1	28.2	31.3	72.8	70.7
	GFDL-ESM4 SSP119	4.1	0.5	-2.3	1.5	1.9	10.9	1.9	-4.5	4.2	5.6
	GFDL-ESM4 SSP270	3.5	2.6	-0.2	6.2	3.6	9.1	7.4	1.9	19.9	12.0
	GFDL-ESM4 SSP585	9.9	2.5	4.0	10.1	6.5	28.9	8.5	15.7	36.3	20.8

Table C3. In the top panel are displayed the monthly anomalies in air temperature (in °C) and precipitation (%) in each of the six CMIP6 scenarios from the Abisko Station and Katterjokk Station datasets, calculated for November to March based on the periods of 2071-2100 and 1985-2014.

		Climate anomalies from the Abisko dataset					Climate anomalies from the Katterjokk dataset				
Climate variable	**CMIP6 scenario**	**January**	**February**	**March**	**November**	**December**	**January**	**February**	**March**	**November**	**December**
Air temperature	CanESM5 SSP119	2.6	3.3	1.5	4.1	3.2	2.6	3.3	1.5	4.1	3.2
	CanESM5 SSP270	5.8	5.3	4.3	6.1	7.0	5.8	5.3	4.3	6.1	7.0
	CanESM5 SSP585	8.5	8.2	6.2	8.7	9.7	8.5	8.2	6.2	8.7	9.7
	GFDL-ESM4 SSP119	1.2	1.7	0.8	1.3	-0.1	1.2	1.7	0.8	1.3	-0.1
	GFDL-ESM4 SSP270	2.8	2.5	2.0	2.5	2.5	2.8	2.5	2.0	2.5	2.5
	GFDL-ESM4 SSP585	5.7	4.3	3.7	4.9	4.3	5.7	4.3	3.7	4.9	4.3
Precipitation	CanESM5 SSP119	-22.4	0.6	12.1	-25.2	17.6	22.4	0.6	12.1	-25.2	17.6
	CanESM5 SSP270	-16.5	14.1	-10.8	-31.3	-8.3	16.5	14.1	-10.8	-31.3	-8.3
	CanESM5 SSP585	4.2	-10.3	-32.3	-48.9	-34.1	-4.2	-10.3	-32.3	-48.9	-34.1
	GFDL-ESM4 SSP119	27.6	-9.2	8.0	-16.1	-9.5	-27.6	-9.2	8.0	-16.1	-9.5
	GFDL-ESM4 SSP270	-2.4	-12.7	12.1	-19.7	-2.9	2.4	-12.7	12.1	-19.7	-2.9
	GFDL-ESM4 SSP585	8.5	11.3	-4.0	-20.1	-7.0	-8.5	11.3	-4.0	-20.1	-7.0

D. Sensitivity analysis

Methodology

Snow properties and processes were first calibrated before evaluating the modelled seasonal dynamics and responses to WWE of snowpack and soil temperature at each site. Hence, site level sensitivity analysis (SA) were conducted to explore the contribution of different parameters and parameter interactions to the estimated snow density, snow depth, snow temperature, and soil temperature during the autumn (October-December) and winter (January-April) seasons, and during specific WWE at each site (except for the tundra site due to lack of observational data for calibration and evaluation). The contribution of the selected parameters was quantified using the variance-based Sobol sensitivity index (Saltelly, 2002; Saltelli and Annoni, 2010). Sobol sensitivity analysis assumes that the model output variations can be decomposed into different subcomponents (Pappas et al., 2008). The main contribution of each parameter to the output variance is quantified by a first-order index, while the overall parameter contribution is quantified by the total-order index, which includes the parameter's interactions with other parameters. In this study, each parameter was sampled 1000 times using the pseudo-random Sobol sequence, while cross-sampling between parameters was done based on the Saltelli method (Saltelli et al. 2008). A plausible range for each parameter was defined based on our current knowledge, literature survey or assigning a certain percentage of changes. The tested parameters and parameter ranges are presented in Table D1. In total, we tested 18.000 simulations for every site (8 parameters) except the "tundra" site due to the limited observational data available. The first-order and total-order Sobol indices for the autumn and winter seasons were calculated based on each simulation's seasonal output average for the period 2001-2010 in the birch forest and fen sites, and for the period 2006-2012 in the peat plateau site. For each site, we compared the modelled snow depth and GT of the 18.000 simulations with observational data from 2001-2010 (2006-2012 in the peat plateau), and selected the parameter values that better depicted each site's seasonal conditions.

In addition, a pre-evaluation of the modelled CO_2 fluxes with the observations using the default quantum efficiency (the rate at which plants convert light into chemical energy; α_{c3}) value (0.08) indicated a large overestimation of both GPP and ER in the tundra site. Hence, we used an α_{c3} value of 0.07 for the tundra PFTs which resulted in more accurately modelled CO_2 fluxes than the default value of 0.08 (Tang et al. 2016).

Table D1. Detailed description of the 8 parameters investigated in the SA, the process in which they are involved, their standard values, and their uncertainty ranges based on the literature or on certain percentage of changes from the original values.

Parameter	Minimum	Maximum	Standard Values	Units	Description
rw_min	0.02	0.06	0.03	Fraction	Minimum fraction of water that can be hold in the snowpack (Anderson et al., 1976)
rw_max	0.1	0.15	0.1	Fraction	Maximum fraction of water that can be hold in the snowpack (Singh et al., 1997)
dens_t	300	550	400	Kg m-3	Maximum density of snow (D'Amboise et al., 2017)
dens_min	50	200	150	Kg m-3	Minimum density of fresh snow (Vionnet et al., 2012)
compaction_rate	0.5	1.5	1	-	Scale factor by which snow compaction is multiplied to either slow down or accelerate the compaction of snow.
ksnow_constant	2	2.44	2.22	-	Empirical constant used to calculate the snow thermal conductivity. Range modified from that of Best et al. (2011) to increase or decrease the snow thermal conductivity up to c. 10%
cnow_constant	0.61	0.77	0.689	-	Empirical constant used to calculate the snow heat capacity. Range modified from that of Fukusako et al. (1990) to increase or decrease the snow heat capacity up to c. 10%
ksnow_constant	1.8	2	1.88	-	Empirical constant used to calculate the snow thermal conductivity. Range modified from that of Best et al. (2011) to increase or decrease the snow thermal conductivity up to ≥ 10%

Results

a) Sobol indices for seasonal output

a) BIRCH FOREST – Autumn 2001 - 2010

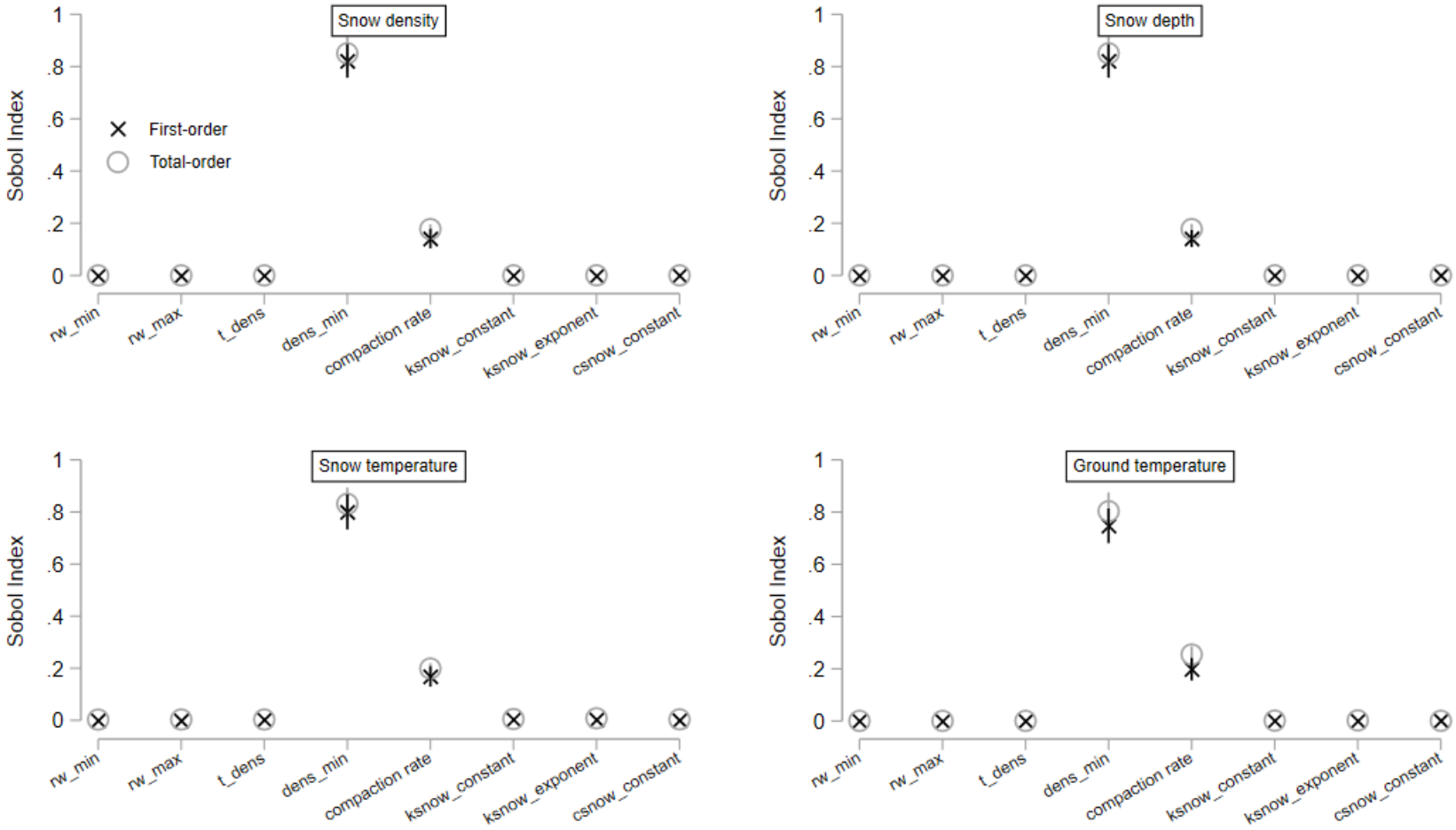

b) BIRCH FOREST – Winter 2001 - 2010

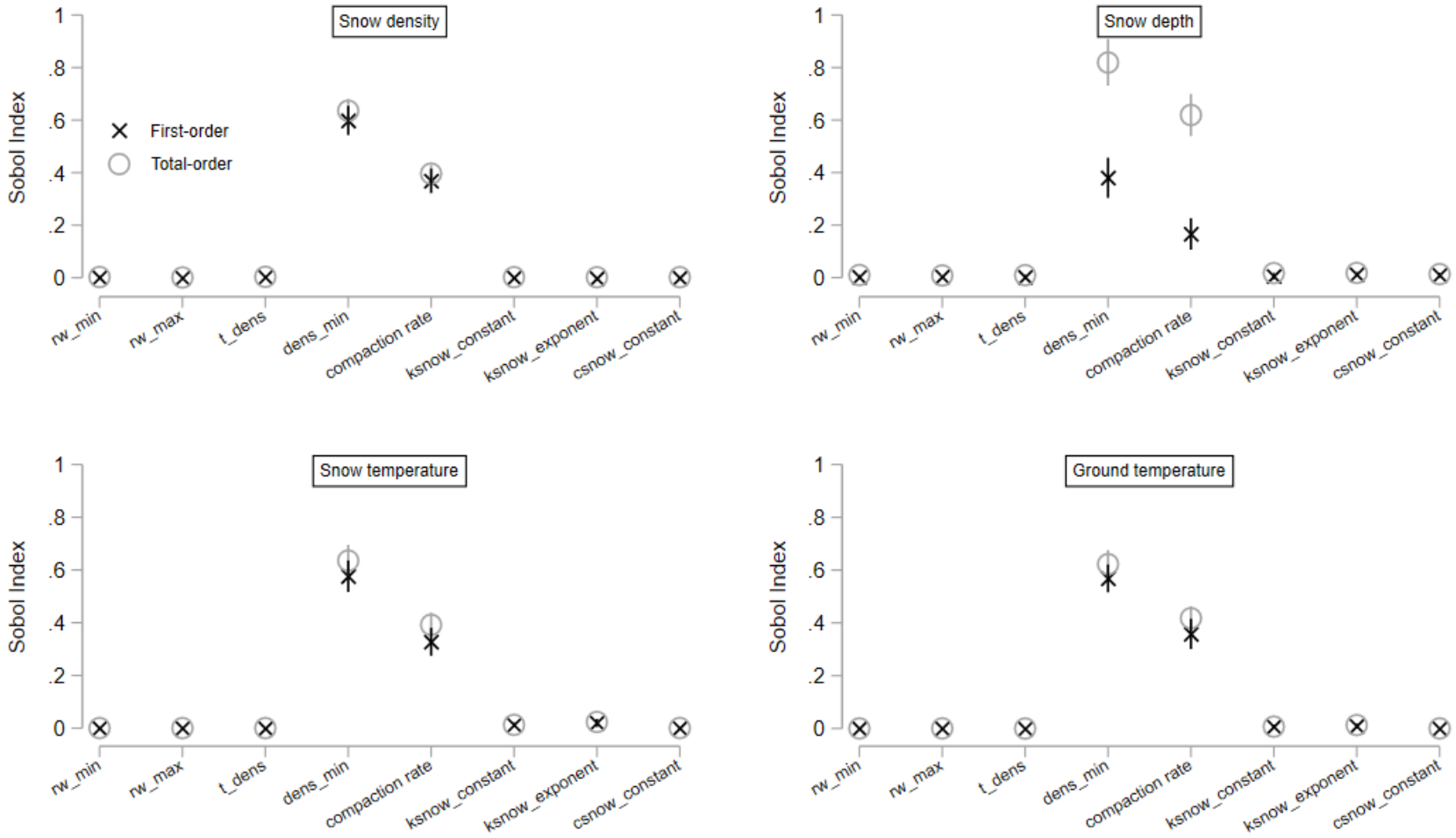

Figure D1. First- and total-order Sobol indices of the eight examined parameters for snow depth, snow density, snow temperature, and ground temperature, at the birch forest, during the autumn (a) and winter seasons (b) in 2001-2010.

a) PEAT PLATEAU – Autumn 2006 – 2012

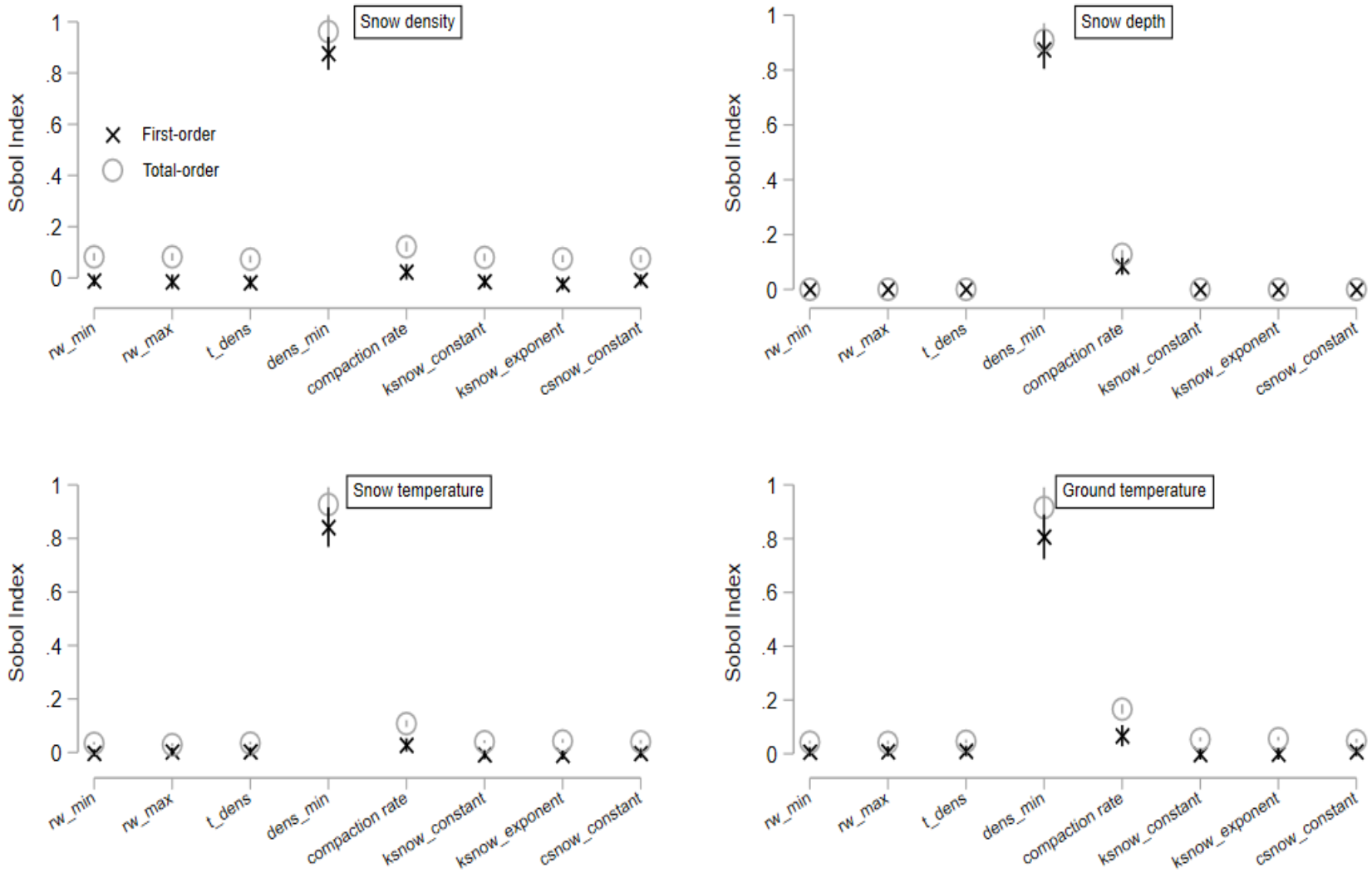

b) PEAT PLATEAU – Winter 2006 – 2012

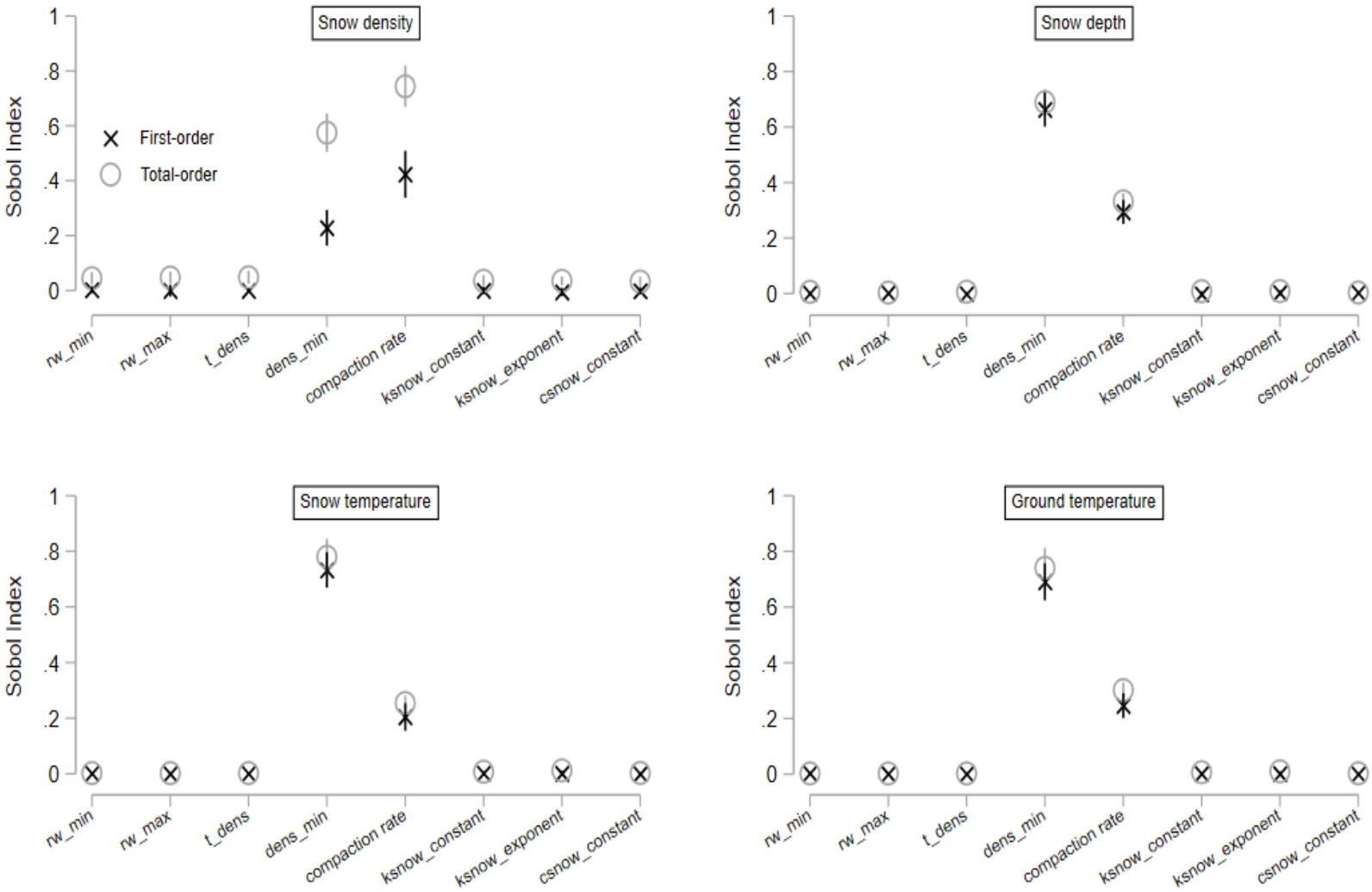

Figure D2. First- and total-order Sobol indices of the eight examined parameters for snow depth, snow density, snow temperature, and ground temperature, at the peat plateau, during the autumn (a) and winter seasons (b) in 2006-2012.

a) FEN – Winter 2001 - 2010

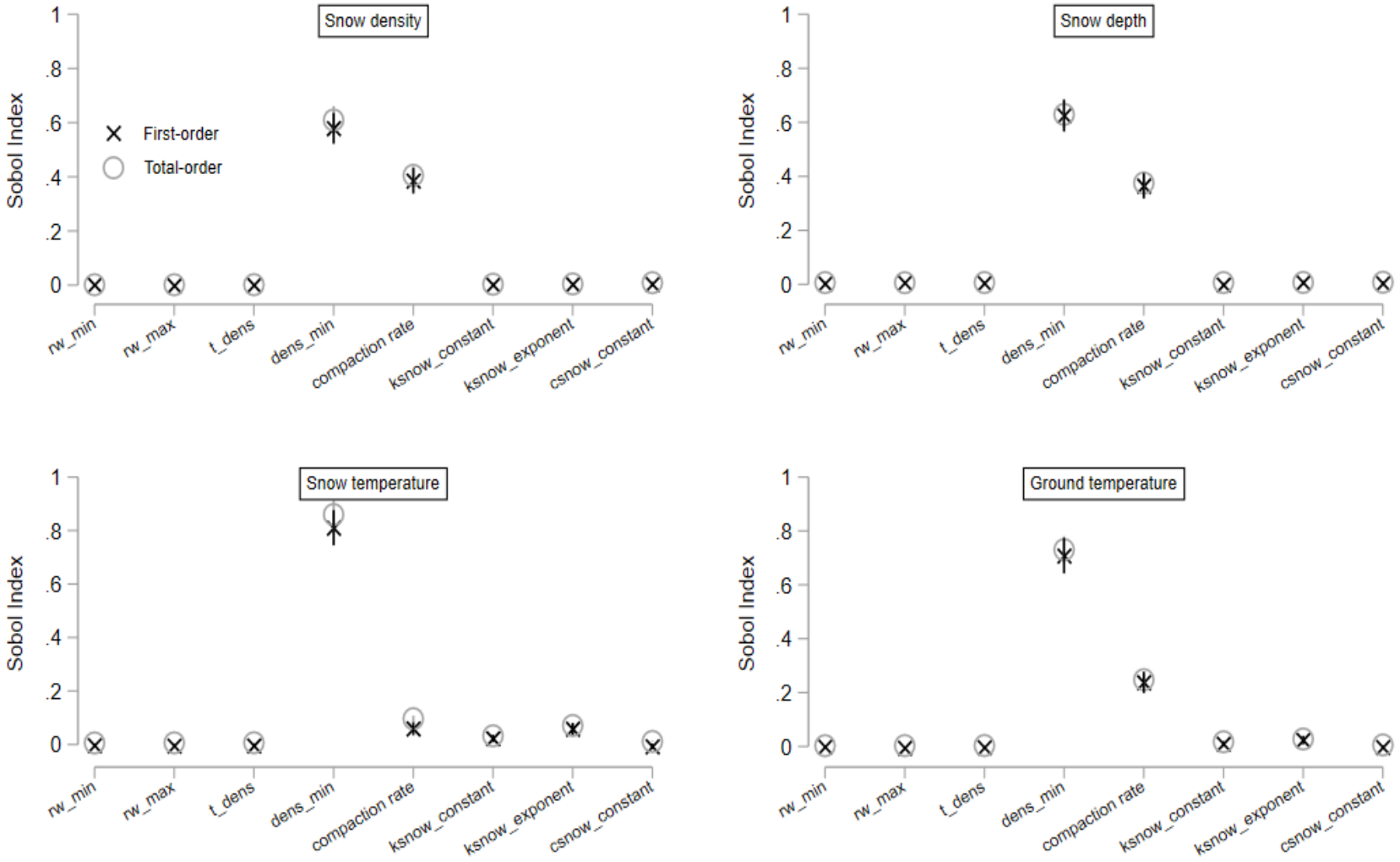

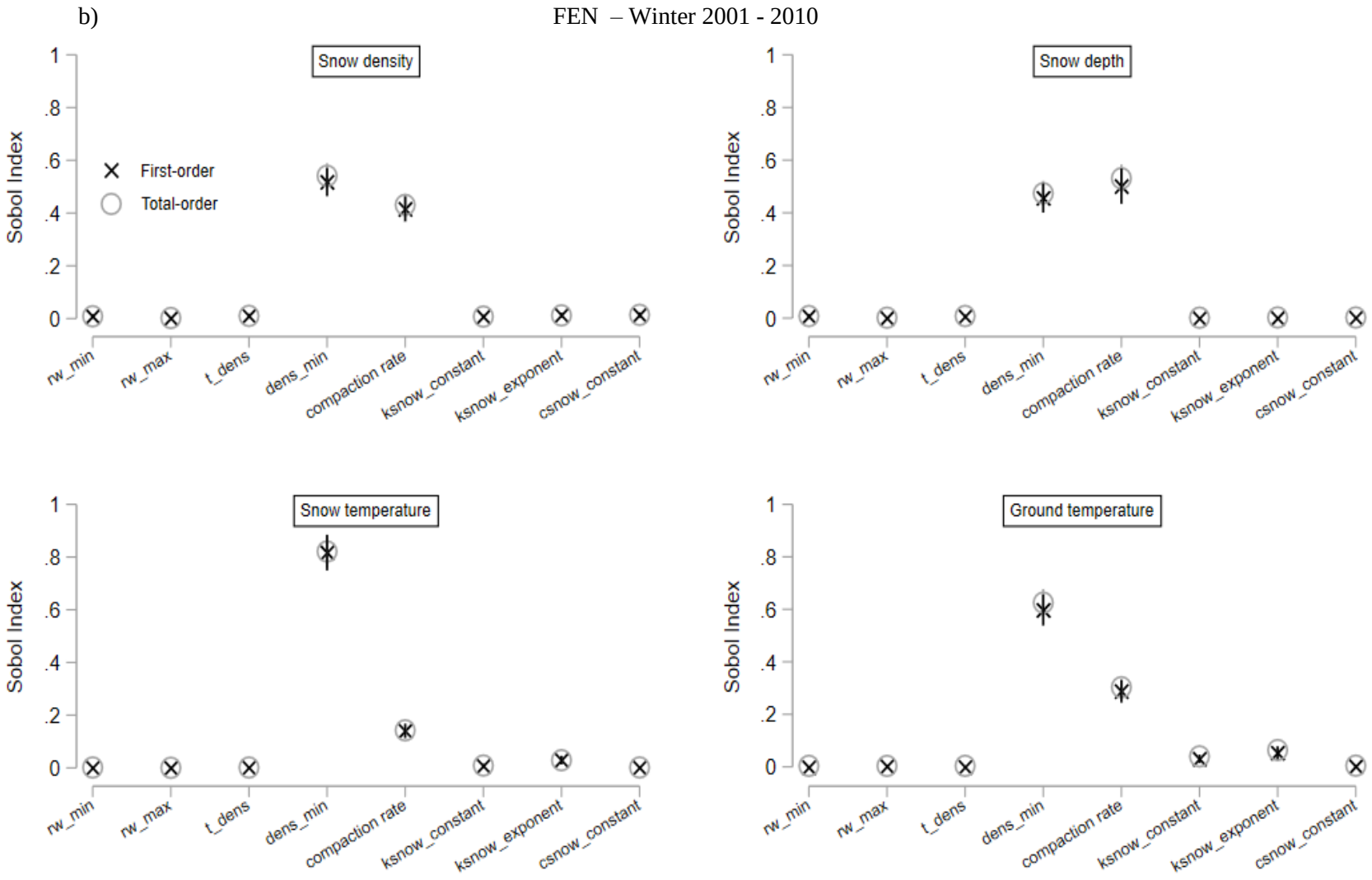

Figure D3. First- and total-order Sobol indices of the eight examined parameters for snow depth, snow density, snow temperature, and ground temperature, at the fen, during the autumn (a) and winter seasons (b) in 2001-2010.

b) Comparing measured vs modelled seasonal values

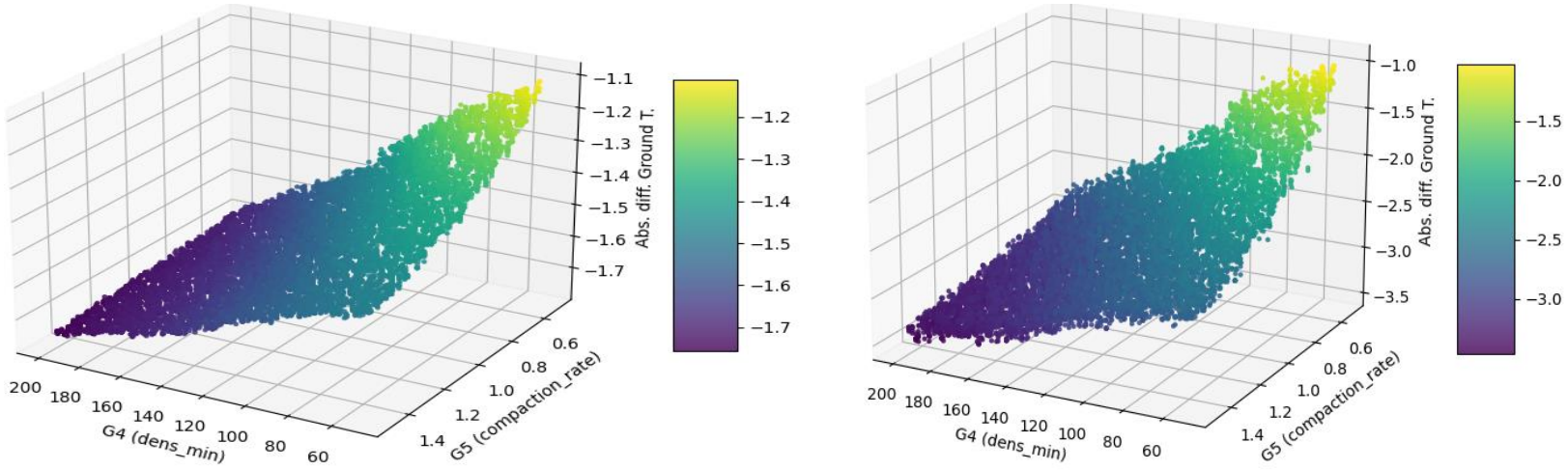

Figure D4. The absolute modelled vs observed difference in ground temperature at the birch forest site, during the autumn (left) and winter (right) seasons in 2001-2010.

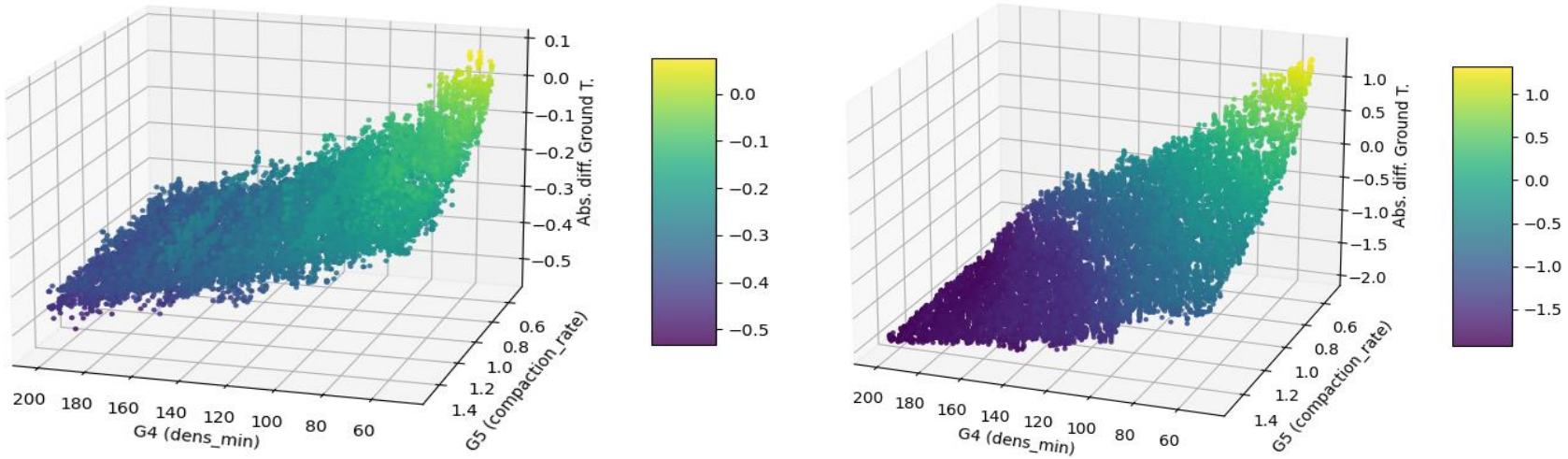

Figure D5. The absolute modelled vs observed difference in ground temperature at the peat plateau site, during the autumn (left) and winter (right) seasons in 2006-2012.

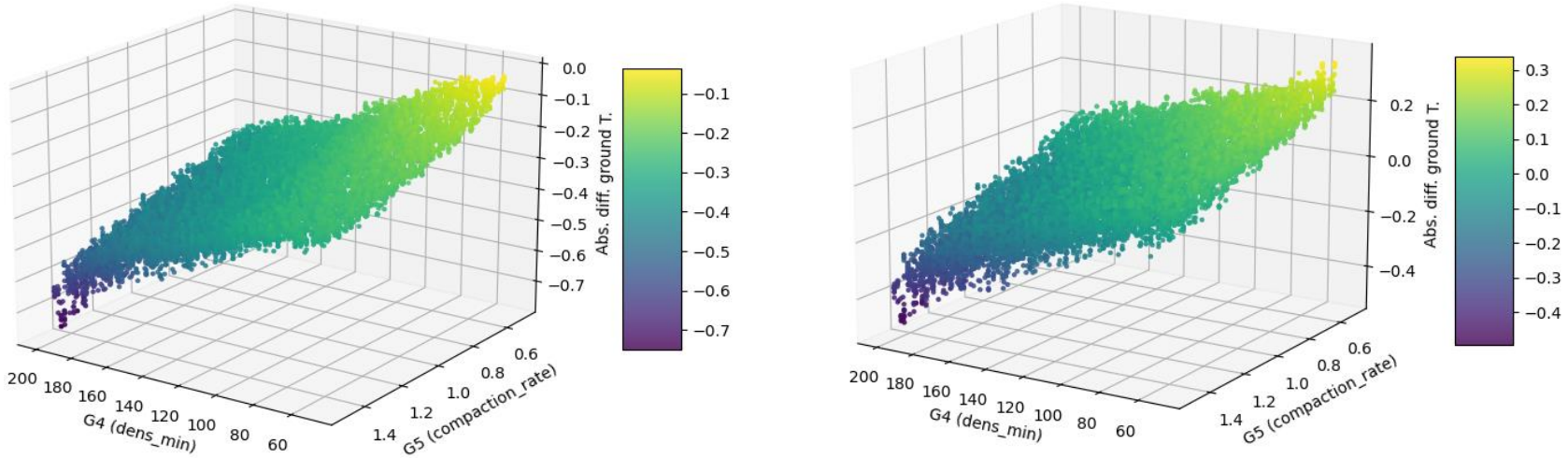

Figure D6. The absolute modelled vs observed difference in ground temperature at the fen site, during the autumn (left) and winter (right) seasons in 2001-2010.

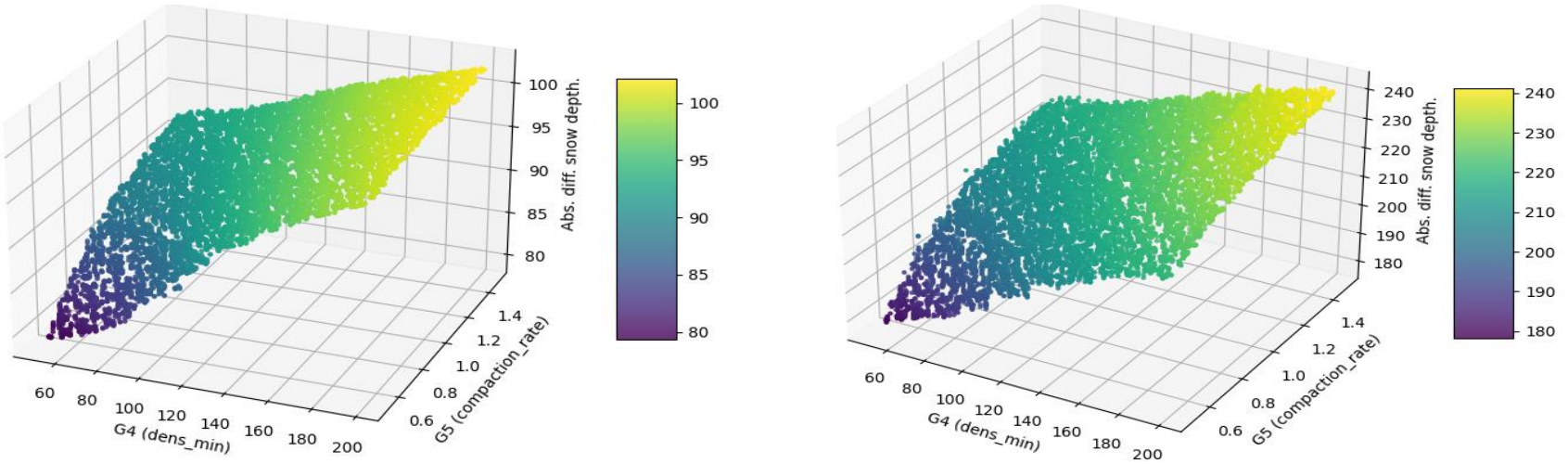

Figure D7. The absolute modelled vs observed difference in snow depth at the birch forest site, during the autumn (left) and winter (right) seasons in 2001-2010.

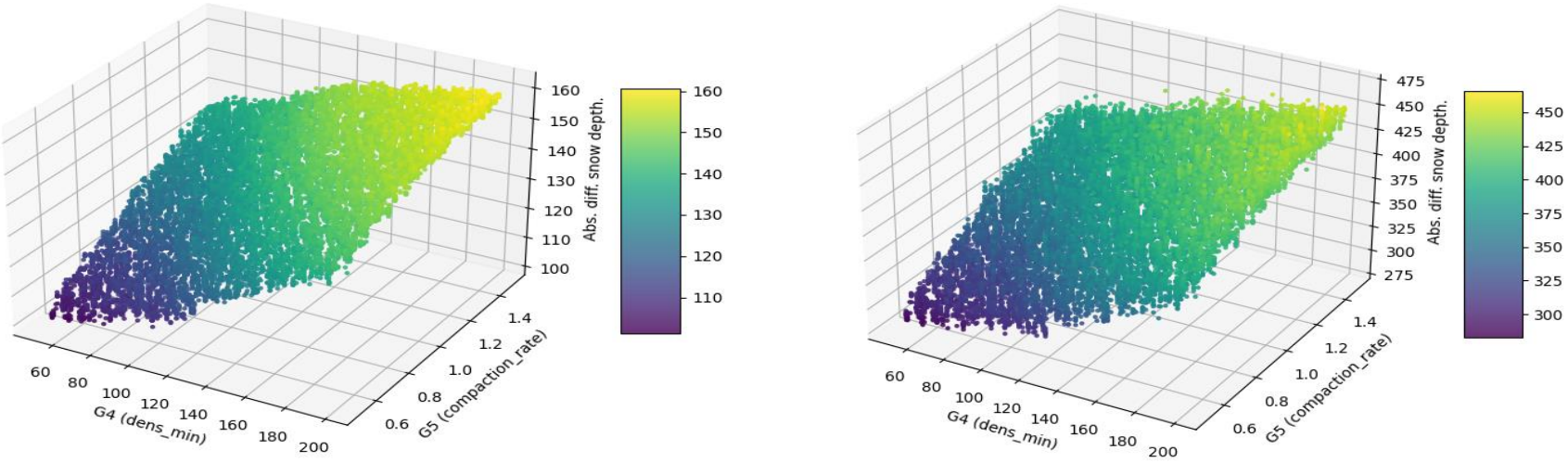

Figure D8. The absolute modelled vs observed difference in snow depth at the fen site, during the autumn (left) and winter (right) seasons in 2001-2010.

E. Model evaluation

Table E1. Full detailes of the observation data from the Torneträsk area used to evaluate model's performance.

Data	Time period	Site	Reference
Snow depth	2011 - 2018	Birch forest, peat plateau, fen	ANS 2020
Ground temperature	2011 - 2018	Birch forest	ANS 2020
Ground temperature	Growing-season 2011	Tundra	A. Michelsen, not published
Ground temperature	2013 - 2018	Peat plateau	M. Johansson, not published
Ground temperature	2019- 2020	Fen	D. Pascual, not published
Eddy Covariance NEE	2007- 2009	Birch forest	(Heliasz, 2012)
Ec-tower measured NEE	2016 - 2018	Peat plateau (from Stordalen)	ICOS 2019
Eddy Covariance NEE	2006 - 2008	Fen (from Stordalen)	(Christensen et al., 2012)
Chamber-measured NEE	Growing season 2010-2012	Tundra	(Finderup Nielsen et al. 2019)
Chamber-measured GPP	Growing season 2010-2012	Tundra	(Finderup Nielsen et al. 2019)
Chamber-measured Reco	Growing season 2010-2012	Tundra	(Finderup Nielsen et al. 2019)
EC-tower measured CH_4	2016 - 2017	Peat plateau (from Stordalen)	ICOS 2019
EC-tower measured CH4	2006 to 2007	Fen (from Stordalen)	(Jackowicz-Korczynski et al., 2010)

Evaluation of physical and biogeochemical variables in the historical period

Evaluation of physical variables

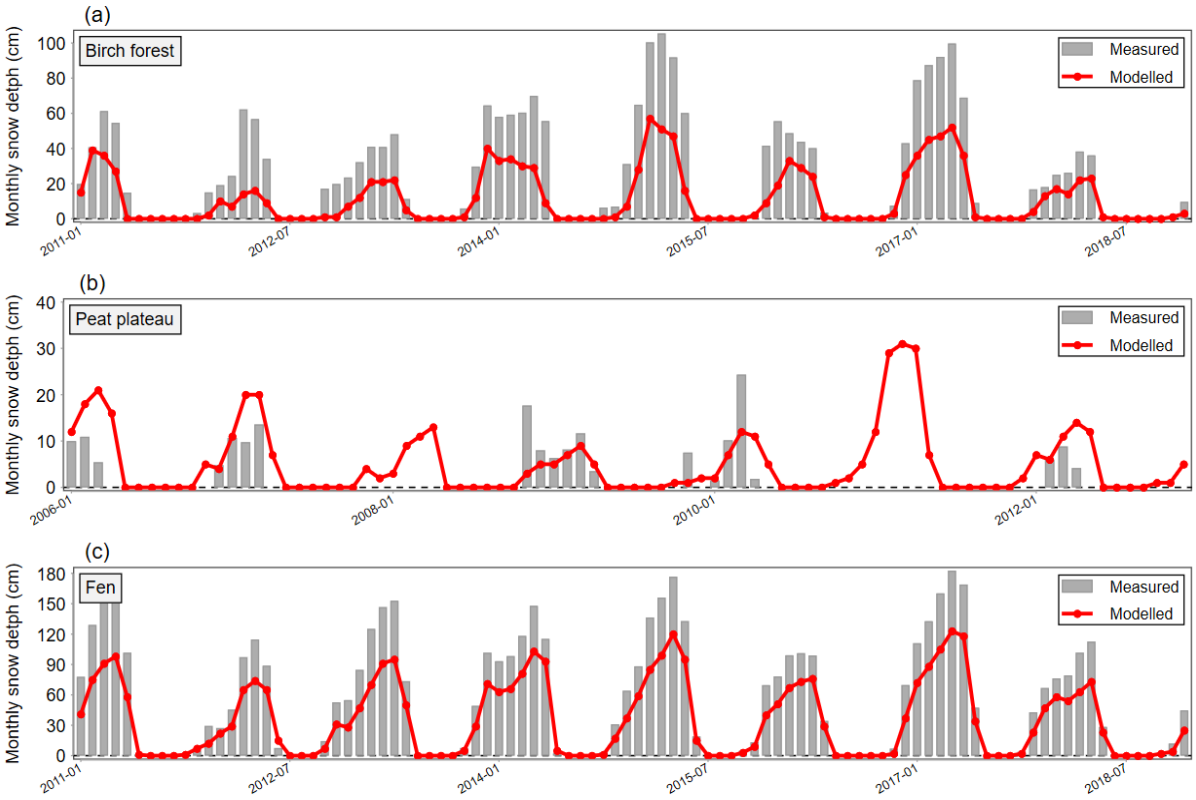

Figure E1. Modeled and measured monthly snow depth at the birch forest (a), peat plateau (b), and fen sites (c). At the peat plateau, the measured data is very scarce and monthly means are based on very few or even single measurements.

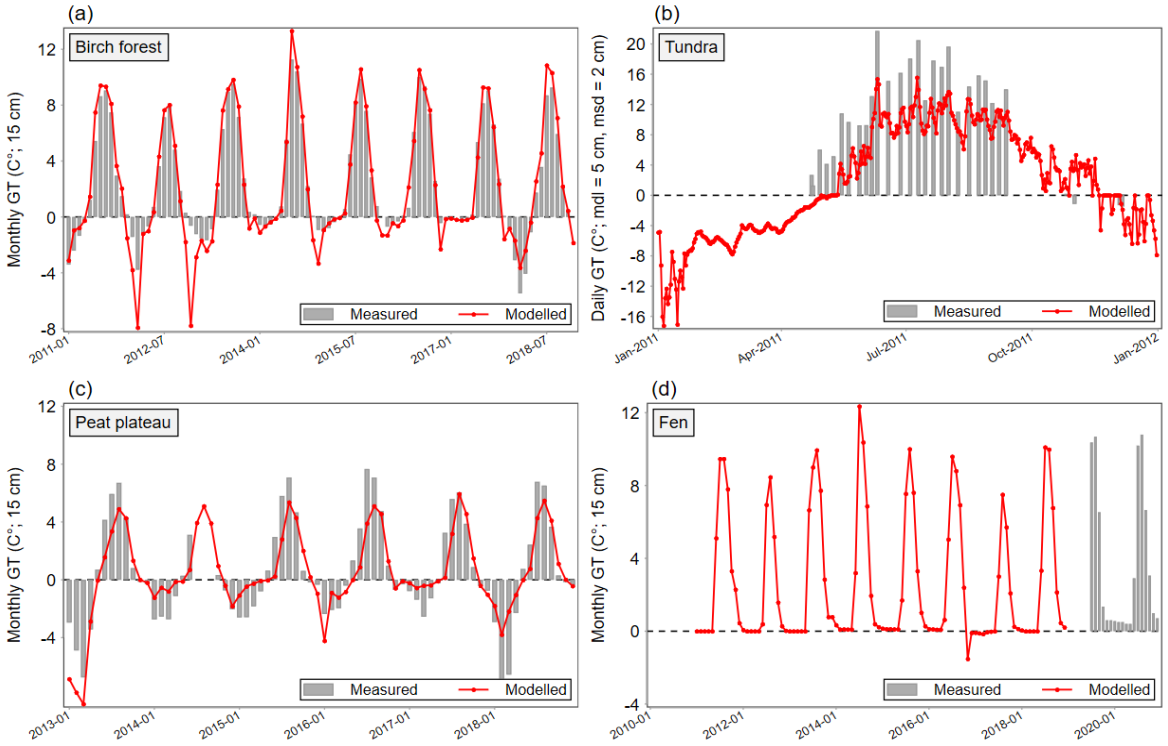

Figure E2. Modeled and measured monthly ground temperatures (GT) at the birch forest (a), peat plateau (c), and fen sites (d), and daily GT in the growing season at the tundra site (b).

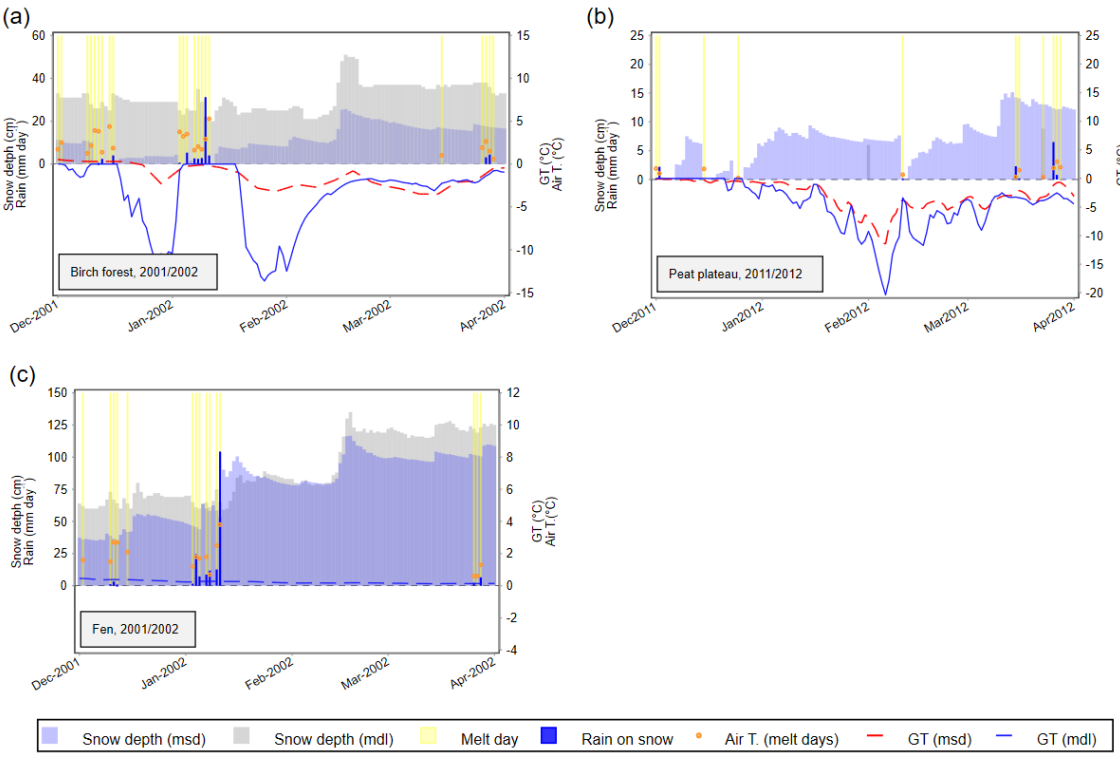

Figure E3. Modelled and measured snow depth and ground temperature from December to March in two of the years with the highest frequencies and intensities of WWE measured in the study area (2002 and 2012; Pascual & Johansson, 2022). Yellow bars and orange dots denote melt days and their measured mean daily air temperature, respectively. Blue bars indicate the occurrence of liquid precipitation (rain) and the measured amounts in mm.

Evaluation of biogeochemical variables

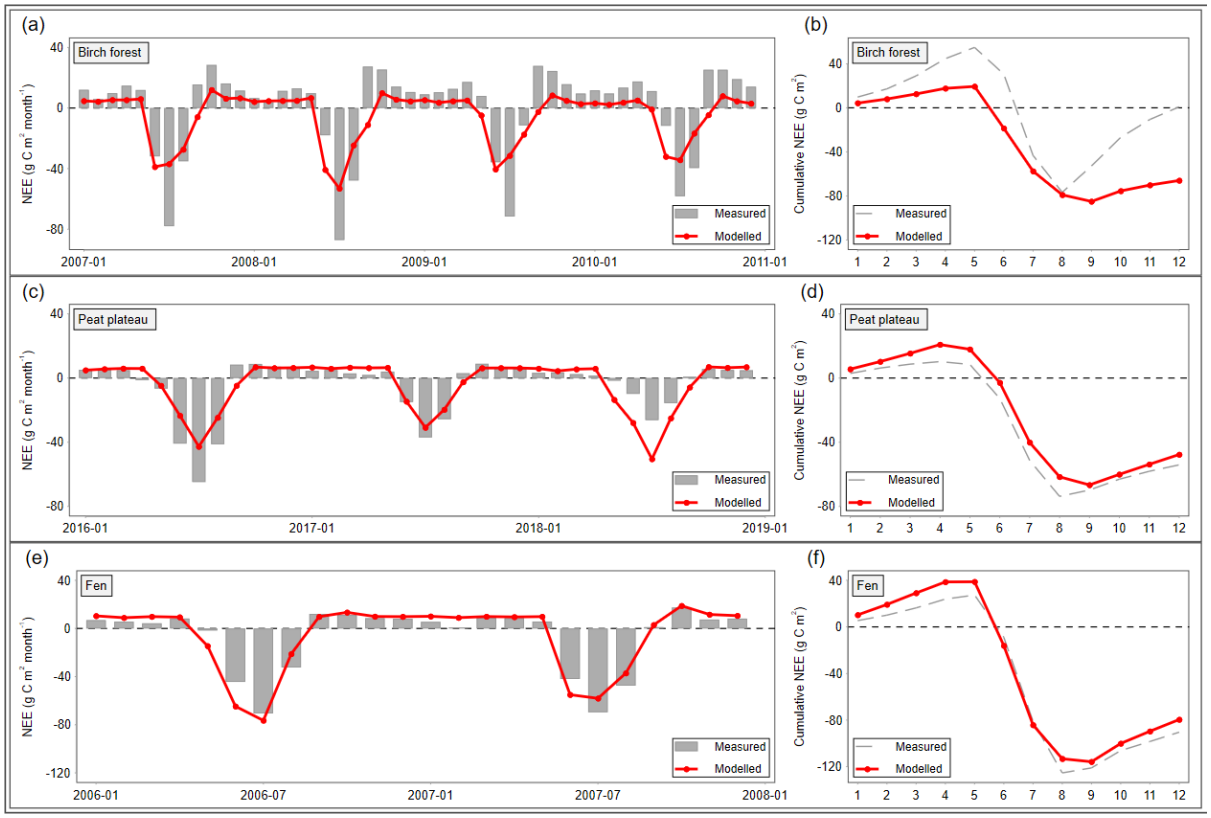

Figure E4. Modelled and measured monthly (left) and mean annual cumulative (right) CO^2 net ecosystem exchange (NEE) fluxes for the birch forest (a-b), tundra (c-d), and peat plateau (e-f) sites. Positive values indicate ecosystem release to the atmosphere and negative values indicate ecosystem uptake.

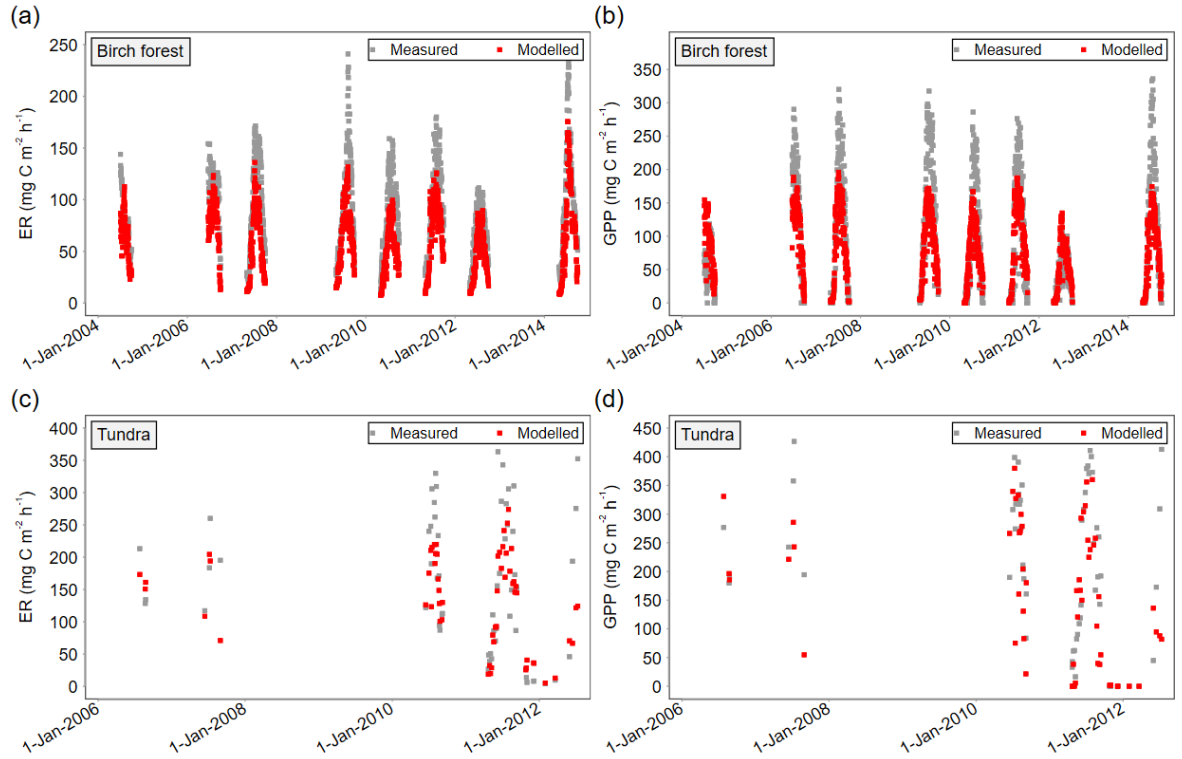

Figure E5. Modeled and measured daily ecosystem respiration (ER; left column) and gross primary production (GPP; right column) in the growing-season at the birch forest (a-b) and tundra (c-d) sites.

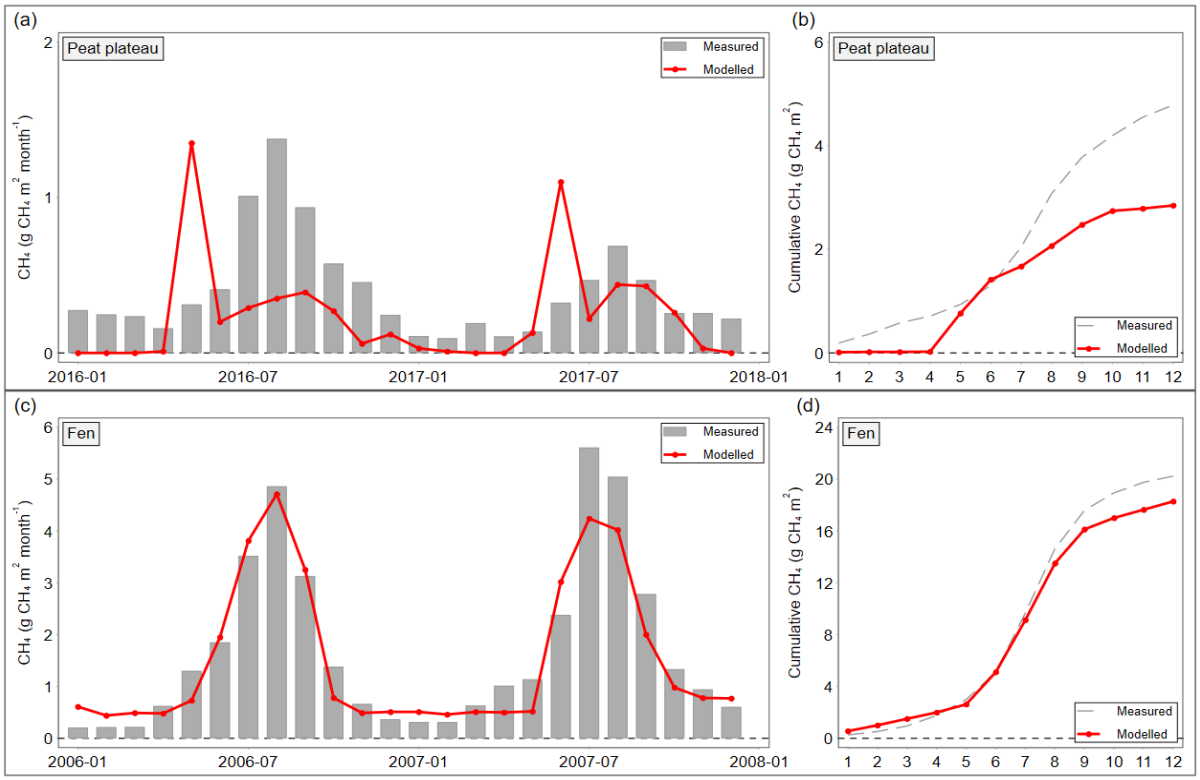

Figure E6. Modelled and measured monthly (left) and mean annual cumulative (right) CH_4 fluxes for the peat plateau (a-b) and fen (c-d) sites.

F. Impacts of WWE on physical variables

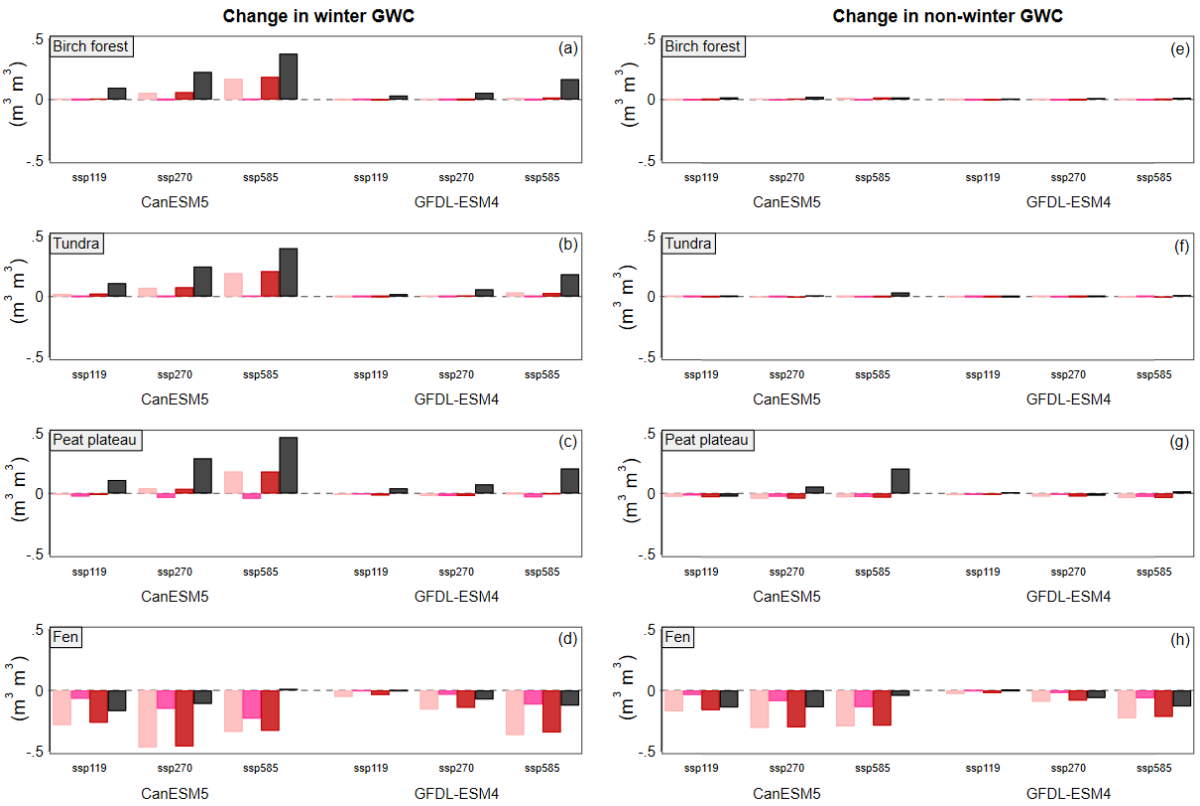

Figure F1. Differences between the model output of the MANIPULATION runs (S1, light pink; S2, pink; S3, red; S4, dark grey) and the HISTORICAL runs (S0), for the variables winter GWC (m^3 m^3; left column), and non-winter GWC (m^3 m^3; right column), at each of the simulated sites. Differences calculated by subtracting each of the MANIPULATION (S1-S4) from the FORCING (S0) simulation outputs.

G. Impacts of WWEs on biogeochemical variables

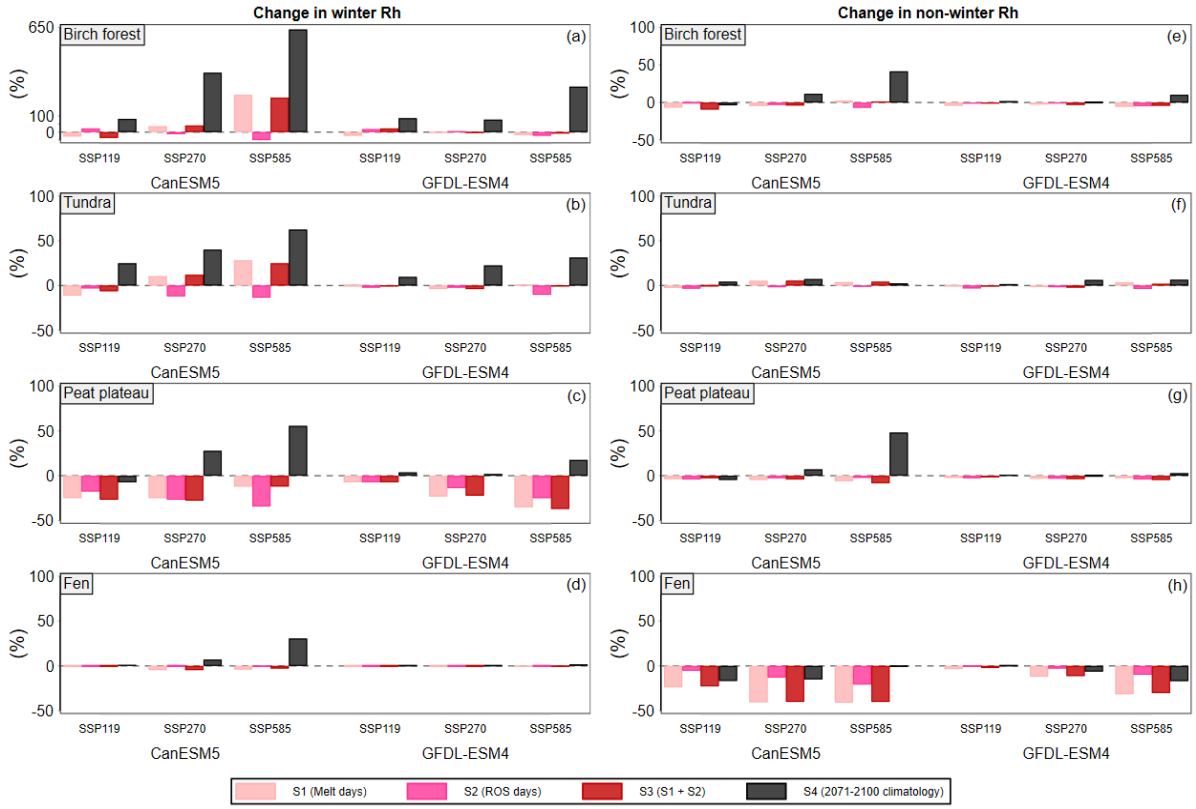

Figure G1. Differences between the model output of the MANIPULATION runs (S1, light pink; S2, pink; S3, red; S4, dark grey) and the HISTORICAL runs (S0)), for the variables winter Rh (%; left column), and non-winter Rh (%; right column), at each of the simulated sites. Differences calculated by subtracting each of the MANIPULATION (S1-S4) from the HISTORICAL (S0) simulation outputs.

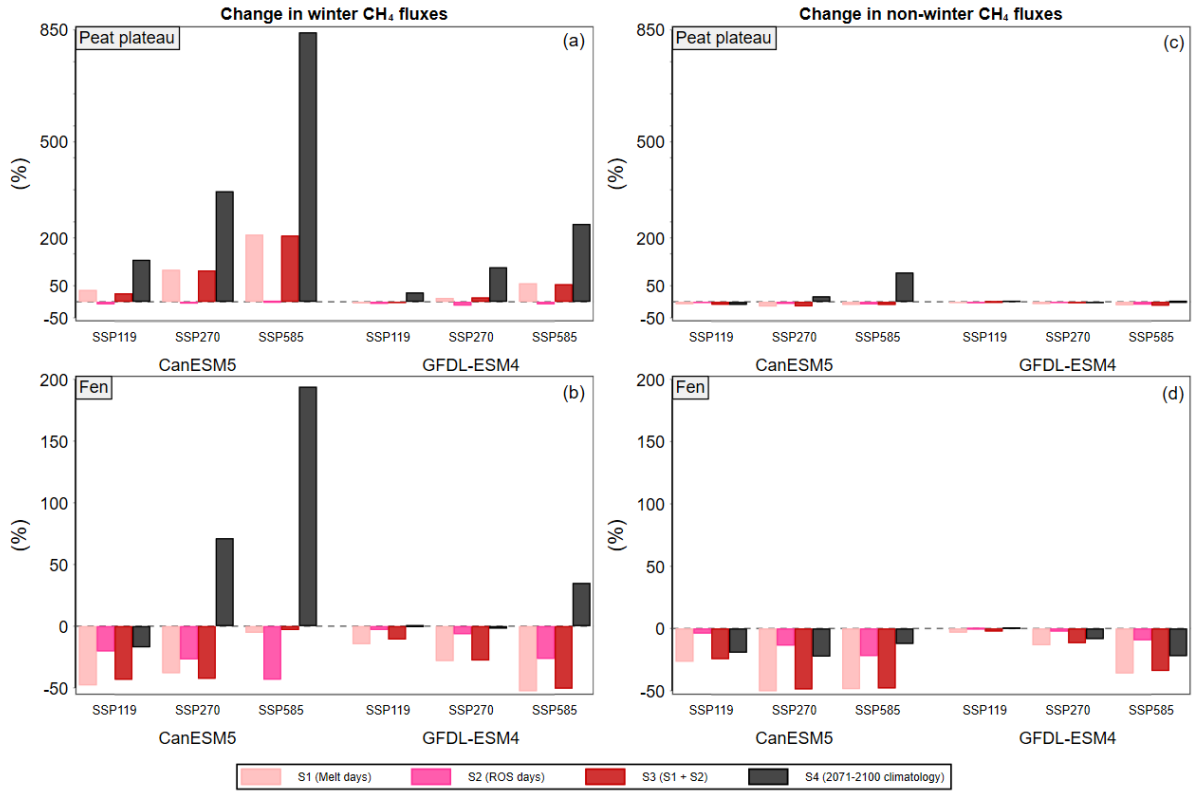

Figure G2. Differences between the model output of the MANIPULATION runs (S1, light pink; S2, pink; S3, red; S4, dark grey) and the HISTORICAL runs (S0), for the variables winter CH_4 and non-winter CH_4 at the peat plateau (a,c) and fen (b,d) sites. Differences calculated by subtracting each of the MANIPULATION (S1-S4) from the HISTORICAL (S0) simulation outputs.

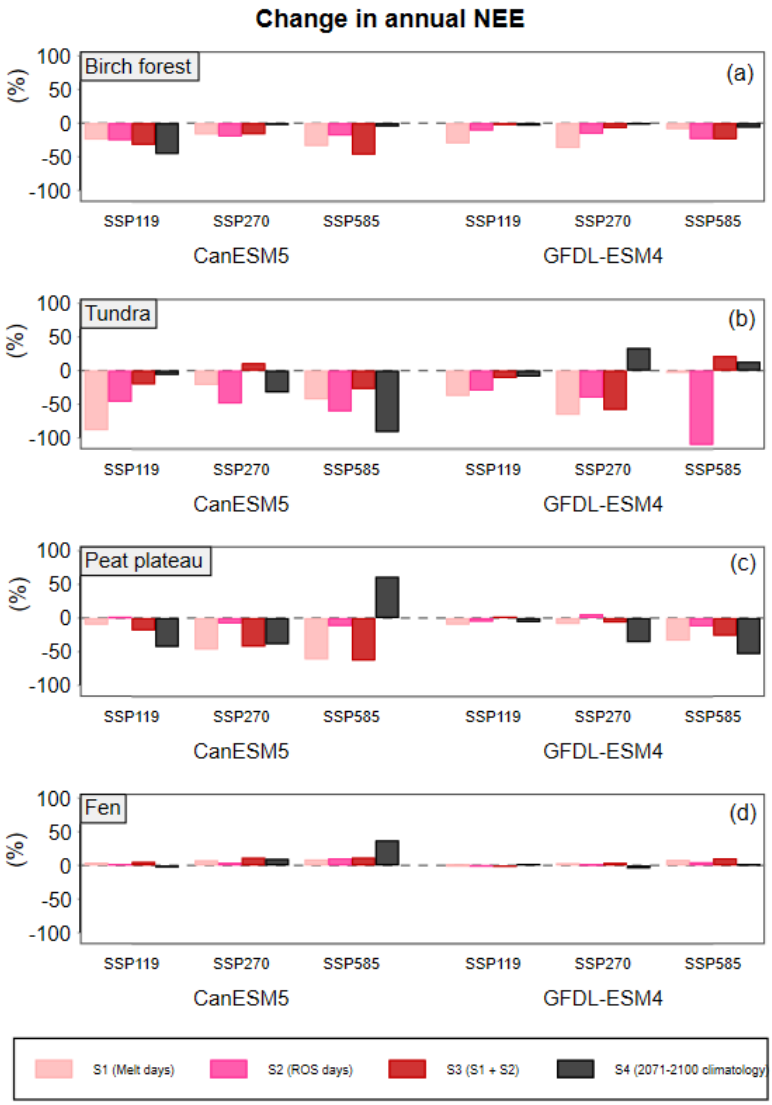

Figure G3. Differences between the model output of the MANIPULATION runs (S1, light pink; S2, pink; S3, red; S4, dark grey) and the HISTORICAL runs (S0), for the variable annual NEE, at the birch forest (a); tundra (b), peat plateau (c), and fen (d) sites. Differences are calculated by subtracting each of the MANIPULATION (S1-S4) from the HISTORICAL (S0) simulation outputs. The positive increases of NEE represent the increases in ecosystem uptake of CO_2, and vice versa.